

## Covalency Effects in KNiF<sub>3</sub>. II. Optical Studies

K. KNOX

*Bell Telephone Laboratories, Murray Hill, New Jersey*

R. G. SHULMAN

*Bell Telephone Laboratories, Murray Hill, New Jersey*

and

*Department of Theoretical Chemistry, Cambridge University, Cambridge, England*

AND

S. SUGANO

*The Institute for Solid State Physics, The University of Tokyo, Azabu Minato ku, Tokyo, Japan*

and

*Bell Telephone Laboratories, Murray Hill, New Jersey*

(Received 14 December 1962)

The optical spectra of KNiF<sub>3</sub> and KMgF<sub>3</sub>:Ni<sup>2+</sup> crystals have been measured between 5000 and 40 000 cm<sup>-1</sup> and from 300 to 4.2°K. Five bands were observed and used to determine three parameters in the ligand field analysis. The cubic crystal field splitting  $10Dq$  was determined to be 7250 cm<sup>-1</sup> and the Racah parameters  $B=955$  cm<sup>-1</sup> and  $C=4230$  cm<sup>-1</sup>. In KNiF<sub>3</sub>, below the Néel temperature of 275°K, there was an average additional shift of 320 cm<sup>-1</sup> to higher energies as compared with the magnetically disordered Ni<sup>2+</sup> in KMgF<sub>3</sub>. This is explained on a molecular field model. An unexpected splitting below  $T_N$  of the  ${}^3A_2 \rightarrow {}^1E$  transition in KNiF<sub>3</sub>, which was not observed in the magnetically dilute crystals has been observed.

### I. INTRODUCTION

THERE are two reasons to study the optical properties of KNiF<sub>3</sub> which is an antiferromagnetic<sup>1,2</sup> below 275°K. First, we need experimental values of the crystalline field strength and the Coulomb interaction parameters to compare with the values calculated in the following paper.<sup>3</sup> Second, we expect fairly large effects of magnetic ordering on the optical spectrum of this crystal because of its high Néel temperature.

In this paper we present experimental studies of the optical spectrum above and below  $T_N$ .

### II. EXPERIMENTAL

Measurements were made on single crystals of KNiF<sub>3</sub>, KMgF<sub>3</sub>:0.10Ni<sup>2+</sup>, KMgF<sub>3</sub>:0.05Ni<sup>2+</sup>, and KMgF<sub>3</sub>:0.01Ni<sup>2+</sup>. The first three crystals were grown in sealed platinum tubes lowered through a temperature gradient, while the KMgF<sub>3</sub>:0.01Ni<sup>2+</sup> was pulled<sup>4</sup> from the melt in a standard germanium crystal puller in which the melt was contained in a quartz crucible. This last method of growing these crystals has been very successful and single crystals 1 in. in diameter and 3 in. long have been grown this way.

At 300°K the edge of the cubic cell<sup>5</sup> is  $(4.014 \pm 0.001)$  Å in KNiF<sub>3</sub> and 4.00 Å in KMgF<sub>3</sub>. The similarity of these dimensions means that Ni<sup>2+</sup> in KMgF<sub>3</sub> should have a very similar environment to Ni<sup>2+</sup> in KNiF<sub>3</sub>, and this is

indeed consistent with our measurements. The major difference between the nickel environment in these two crystals is the existence of a strong magnetic exchange interaction in KNiF<sub>3</sub>.

All measurements were made by Miss D. Dodd with a Carey Model 14 Spectrophotometer operating in the range 5000 to 45 000 cm<sup>-1</sup>. The resolution of the spectrometer with the slits used was  $\sim 15$  cm<sup>-1</sup> in the vicinity of 15 000 cm<sup>-1</sup>. Samples were placed in the refrigerant in one path of this split beam spectrophotometer.

The optical spectra obtained at 4.2, 77, and 300°K for KMgF<sub>3</sub>:0.10Ni<sup>2+</sup> are shown in Fig. 1 and for KNiF<sub>3</sub> in Fig. 2. There is a change in the rate of sweeping through the spectra at 7200 Å. In all the spectra the same five distinct absorption bands are resolved. In Table I we have presented along with the symmetry assignment of the excited states, the frequencies of

TABLE I. The observed frequencies and relative intensities of the absorption peaks of KNiF<sub>3</sub> and KMgF<sub>3</sub>:0.10Ni<sup>2+</sup> at various temperatures, along with the symmetry assignment of the transitions.

Transitions	300°K		77°K		4.2°K	
	$\nu$ (cm <sup>-1</sup> )	Int.	$\nu$ (cm <sup>-1</sup> )	Int.	$\nu$ (cm <sup>-1</sup> )	Int.
${}^3A_2 \rightarrow$	KNiF <sub>3</sub>					
${}^3T_2$	7250	6	7690	5	7650	4
${}^3T_1$	12 530	11	13 230	7	13 230	6
${}^1E$	15 440	0.4	15 810	0.6	15 800	0.6
			16 170 <sup>a</sup>		16 190 <sup>a</sup>	
${}^1T_2$	20 920	0.8	21 670	1.0	21 600	1.0
${}^3T_1$	23 810	23	24 390	12	24 390	12
${}^3A_2 \rightarrow$	KMgF <sub>3</sub> :0.10Ni <sup>2+</sup>					
${}^3T_2$	7380	4	7620	4	7620	
${}^3T_1$	12 820	6	13 160	5	13 160	
${}^1E$	15 530	0.1	15 580	0.1	15 600	
${}^1T_2$	21 190	0.4	21 500	0.5	21 500	
${}^3T_1$	24 140	16	24 400	10	24 450	

<sup>a</sup> This is an extra line appearing at  $T < T_N$ .

<sup>1</sup> R. L. Martin, R. S. Nyholm, and N. C. Stephenson, *Chem. Ind. (London)* **1956**, 83 (1956).

<sup>2</sup> K. Hirakawa, K. Hirakawa, and T. Hashimoto, *J. Phys. Soc. Japan* **15**, 2063 (1960).

<sup>3</sup> S. Sugano and R. G. Shulman, following paper [*Phys. Rev.* **130**, 517 (1963)].

<sup>4</sup> P. Freeland (private communication).

<sup>5</sup> A. Okazaki and Y. Suemune, *J. Phys. Soc. Japan* **16**, 671 (1961).

these band peaks in  $\text{cm}^{-1}$  at 300, 77, and  $4.2^\circ\text{K}$  for  $\text{KNiF}_3$  and  $\text{KMgF}_3:0.10\text{Ni}^{2+}$ . Between 300 and  $77^\circ\text{K}$  the band peaks shift to higher energy, while between 77 and  $4.2^\circ\text{K}$  no shift is discernible. By comparing the band peak at  $300^\circ\text{K}$  with the values measured at  $77^\circ\text{K}$  we have determined the shift,  $\Delta\nu$ , for each band. The shifts in  $\text{KNiF}_3$ , which becomes antiferromagnetic at  $275^\circ\text{K}$ , are significantly different from those in the dilute crystal, which presumably does not become ordered in the temperature range studied. The difference is clearly shown in Table II. These shifts are discussed in the following section in terms of contributions from lattice vibrations and the magnetic exchange energy.

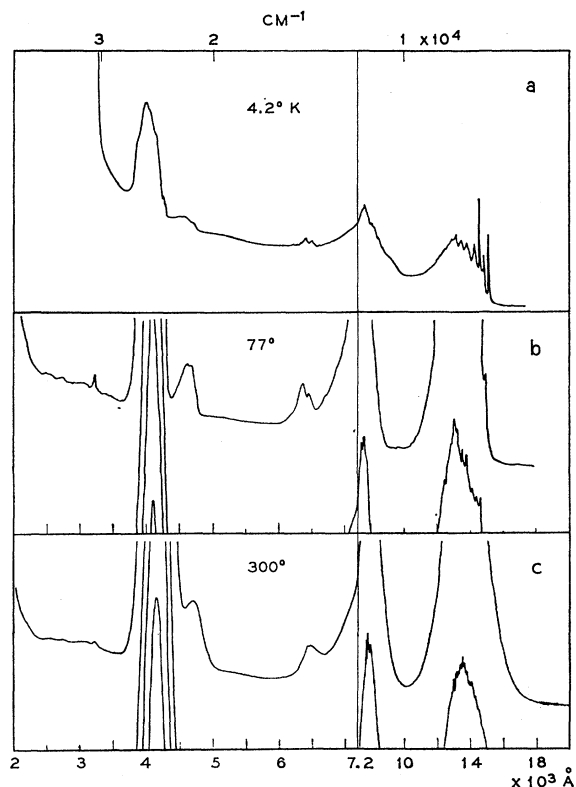


FIG. 1. The absorption spectra of  $\text{KMgF}_3:0.10\text{Ni}^{2+}$  at 4.2, 77, and  $300^\circ\text{K}$  are shown in parts (a), (b), and (c), respectively. Ångstrom units are plotted at the bottom and  $\text{cm}^{-1}$  at the top. Notice the change of scale at  $7200 \text{ Å}$ .

The band near  $16000 \text{ cm}^{-1}$  has two peaks at 77 and  $4.2^\circ\text{K}$  in  $\text{KNiF}_3$ , while in  $\text{KMgF}_3:\text{Ni}^{2+}$  it has a single main peak. A detailed spectrum of this band in  $\text{KNiF}_3$

TABLE II. Band peak shifts in  $\text{KNiF}_3$  and  $\text{KMgF}_3:\text{Ni}^{2+}$ . The units are  $\text{cm}^{-1}$ .

	$\Delta\nu(\text{KNiF}_3)$	$\Delta\nu(\text{KMgF}_3:\text{Ni}^{2+})$	Difference
${}^3A_2 \rightarrow {}^3T_2$	440	240	200
$\rightarrow {}^3T_1$	700	340	360
$\rightarrow {}^1E$	370	50	320
$\rightarrow {}^1T_2$	750	310	440
$\rightarrow {}^3T_1$	580	260	320

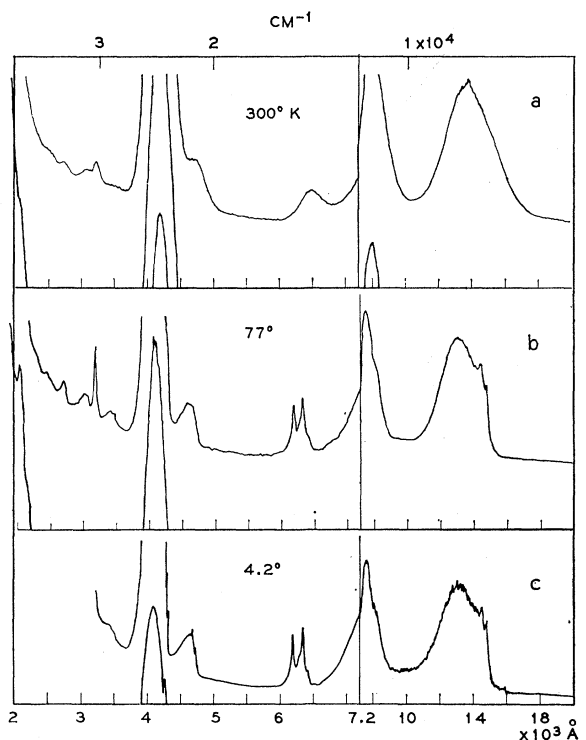


FIG. 2. The absorption spectra of  $\text{KNiF}_3$  at 4.2, 77, and  $300^\circ\text{K}$  are shown in parts (c), (b), and (a), respectively.

at  $4.2^\circ\text{K}$  is shown in Fig. 3(b). For comparison, the same band in  $\text{KMgF}_3:0.10\text{Ni}^{2+}$  is shown in Fig. 3(a) at  $77^\circ\text{K}$  which did not differ from the  $4.2^\circ\text{K}$  measurements. As clearly seen in Fig. 3, all the small peaks in the dilute crystal, denoted by A through E, can be correlated with those in  $\text{KNiF}_3$  denoted by the same letters. An intense extra line towards shorter wavelengths remains unidentified in  $\text{KNiF}_3$ . To investigate the possibility that the small peaks of the  $16000 \text{ cm}^{-1}$  band in  $\text{KMgF}_3:\text{Ni}^{2+}$  arose from  $\text{Ni}^{2+}$  pairs, grouped together as nearest neighbors, we have also measured the spectrum of  $\text{KMgF}_3:0.05\text{Ni}^{2+}$  where the  $16000$

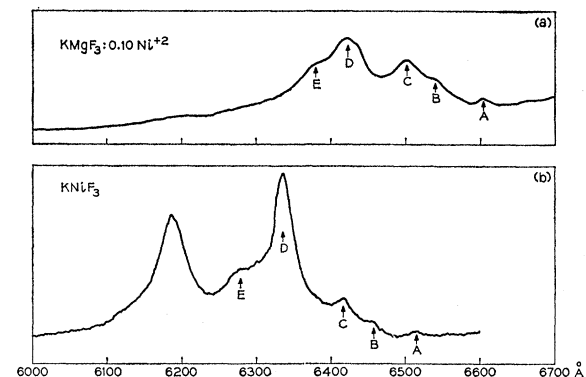


FIG. 3. (a) The  ${}^3A_2 \rightarrow {}^1E$  band in  $\text{KMgF}_3:0.10\text{Ni}^{2+}$  at  $77^\circ\text{K}$  which was identical with the spectra observed at  $4.2^\circ\text{K}$ . (b) The  ${}^3A_2 \rightarrow {}^1E$  band in  $\text{KNiF}_3$  at  $4.2^\circ\text{K}$ .

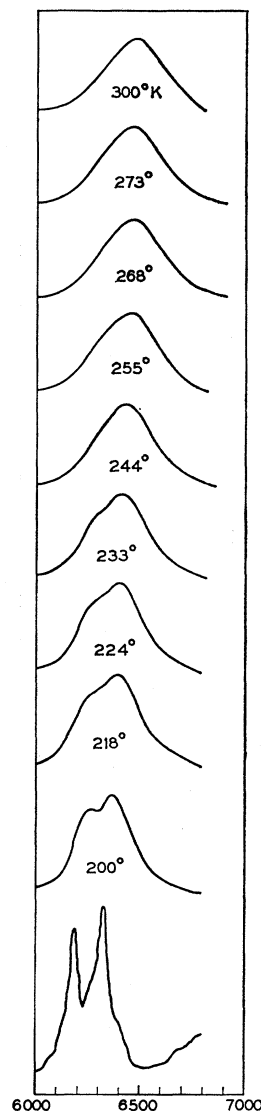


FIG. 4. The  ${}^3A_2 \rightarrow {}^1E$  band in  $\text{KNiF}_3$  as a function of temperature. The bottom trace was observed at  $77^\circ\text{K}$ . Notice that the shorter wavelength peak changes more rapidly with temperature than the other.

$\text{cm}^{-1}$  band looked the same, thereby eliminating the possibility that those peaks were caused by  $\text{Ni}^{2+}$ - $\text{Ni}^{2+}$  pairs. It can be seen from Table I, where the relative oscillator strengths are plotted vs temperature, that the  $16\,000\text{ cm}^{-1}$  band in  $\text{KNiF}_3$  is the only band whose strength definitely increased as the temperature was lowered from  $300$  to  $77^\circ\text{K}$  (the small apparent increase in intensity of the  $21\,000\text{ cm}^{-1}$  band is inaccurate because of the strong overlapping  $24\,000\text{ cm}^{-1}$  band). This critical temperature range was studied in  $\text{KNiF}_3$  more carefully with the results shown in Fig. 4. The splitting into the doublet first becomes apparent in the region of  $T_N$ . A small hump appears on the high-frequency shoulder of the main peak, and, when the temperature is further decreased, the intensity of the hump increases while its peak shifts towards higher frequency. The increase of the total intensity of the band is equal to the intensity of this extra line below

TABLE III. Energies of lowest excited states.

States	Energies
${}^3A_2$	$0$
${}^3T_2$	$\Delta$
$({}^1E_g e^g) + ({}^1E_g e^g)$	${}^3T_1$
$({}^1E_g e^g) + ({}^1E_g e^g)$	${}^3T_1$
$({}^1E_g e^g) + ({}^1E_g e^g)$	${}^1E$
$({}^1E_g e^g) + ({}^1E_g e^g)$	${}^1T_2$
$({}^1E_g e^g) + ({}^1E_g e^g)$	${}^1A_1$
	$15B/2 + 3\Delta/2 - \frac{1}{3}[(9B - \Delta)^2 + 144B^2]^{1/2}$
	$15B/2 + 3\Delta/2 + \frac{1}{3}[(9B - \Delta)^2 + 144B^2]^{1/2}$
	$17B/2 + 2C + \Delta - \frac{1}{3}[(B + 2\Delta)^2 + 48B^2]^{1/2}$
	$17B/2 + 2C + 3\Delta/2 - \frac{1}{3}[(B + \Delta)^2 + 48B^2]^{1/2}$
	$17B + 9C/2 + \Delta - \frac{1}{3}[(2B + C + 2\Delta)^2 + 24(2B + C)^2]^{1/2}$

$T_N$ . At  $4.2^\circ\text{K}$  the extra line is located  $390\text{ cm}^{-1}$  from the original peak.

### III. DISCUSSION

#### A. Determination of Parameters

The well-resolved absorption bands allow a good test of the theory of the excited states of  $\text{Ni}^{2+}$  in an octahedral environment. Fortunately, the theory is well developed. Ignoring spin-orbit interaction, analytical expressions for the energy of the excited states of interest are obtained by using Tanabe and Sugano's<sup>6</sup> matrix elements as shown in Table III.

A numerical expression for the energy, including the effects of the spin-orbit interaction, has been made available by Liehr and Ballhausen.<sup>7</sup> In their expression the energy is numerically given over a fairly wide range of the parameters  $\Delta$ ,  $B$ ,  $C$ , and  $\lambda$ ; where  $\lambda$  is the coupling constant of the spin-orbit interaction,  $\Delta$  is the cubic field parameter usually written as  $10Dq$ , and  $B$  and  $C$  are Racah's Coulomb interaction parameters corresponding to Slater integrals,  $F_2$  and  $F_4$ .

For determining the parameter values it is necessary to decide which temperature should be used as the band peaks shift with temperature. In order to avoid ambiguities associated with the effects of spin ordering upon the positions of the absorption bands, we shall use the data taken at  $300^\circ\text{K}$  which is above  $T_N$ .

A trial fit was made, with Liehr and Ballhausen's calculation (Fig. 5), to a set of parameters in which  $F_2 = 14F_4 = 1540\text{ cm}^{-1}$  ( $B = 990\text{ cm}^{-1}$ ,  $C = 3850\text{ cm}^{-1}$ ,  $C/B = \gamma = 3.9$ ),  $\Delta = 7250\text{ cm}^{-1}$ , and  $\lambda = -250\text{ cm}^{-1}$ . The value of  $\lambda$  used came from an electron spin resonance measurement of  $g = 2.28$  for  $\text{Ni}^{2+}$  in  $\text{KMgF}_3$  by Walsh.<sup>8</sup> As seen in Fig. 5 the agreement is good, but the small value of  $\gamma = 3.9$  compared with the free-ion value,  $\gamma_{\text{free}} = 4.7$ , looks unreasonable. It comes from an arbitrary choice of the parameters from the limited set available.

Since this trial shows us the unimportance of the spin-orbit interaction in the parameter range of interest, we have finally determined the parameters by using the analytical expressions of Table III. The absorption peak  ${}^3A_2 \rightarrow {}^3T_2$  determined  $\Delta$ , and those of  ${}^3A_2 \rightarrow {}^3T_1$  and  ${}^3A_2 \rightarrow {}^1E$  determined  $B$  and  $C$ , respectively. The

<sup>6</sup> Y. Tanabe and S. Sugano, J. Phys. Soc. Japan **9**, 753 (1954).

<sup>7</sup> A. D. Liehr and C. J. Ballhausen, Ann. Phys. (N. Y.) **6**, 134 (1959); and (private communication).

<sup>8</sup> W. M. Walsh, Jr., (private communication).

TABLE IV. Comparison between the observed positions of the absorption peaks and the calculation with  $\Delta=7250 \text{ cm}^{-1}$ ,  $B=955 \text{ cm}^{-1}$ , and  $C=4234 \text{ cm}^{-1}$  ( $\gamma=4.4$ ). The spin-orbit interaction is neglected.

Transitions	Calculation ( $\text{cm}^{-1}$ )	Observation ( $\text{cm}^{-1}$ )
${}^3A_2 \rightarrow$		
${}^3T_2$	7250	7250
${}^3T_1$	12 270	12 530
${}^3T_1$	23 810	23 810
${}^1E$	15 430	15 440
${}^1T_2$	22 190	20 920
${}^1A_1$	24 240	...

parameter values thus determined are

$$\Delta=7250 \text{ cm}^{-1}, \quad B=955 \text{ cm}^{-1}, \quad \text{and} \quad C=4234 \text{ cm}^{-1},$$

which give a reasonable value of  $\gamma=4.4$ . Table IV shows comparison between the calculation and experiment. The  $B$  value is reduced from the free-ion value of  $1030 \text{ cm}^{-1}$  by 7%, while  $C$  is reduced from the estimated value of  $4850 \text{ cm}^{-1}$  in the free ion by  $\sim 13\%$ .

### B. The Frequency Shift below $T_N$

As pointed out previously, a remarkable difference between the absorption spectra of  $\text{KNiF}_3$  and  $\text{KMgF}_3$ :  $\text{Ni}^{2+}$  lies in the shifts of the absorption band peaks with decreasing temperature: The shift is much larger in  $\text{KNiF}_3$  than in  $\text{KMgF}_3$ :  $\text{Ni}^{2+}$ . The shift in the dilute crystal is considered to be that usually found in paramagnetic materials. It is probably caused by the thermal contraction of a crystal lattice with decreasing temperature and the interaction of chromophoric electrons with lattice vibrations. In  $\text{KNiF}_3$  a shift of this type is also expected, but the spin ordering below  $T_N$  could produce an additional frequency shift of another type. Such a frequency shift due to spin ordering has been observed by Tsujikawa<sup>9</sup> in  $\text{MnCl}_2 \cdot 4\text{H}_2\text{O}$  and  $\text{MnBr}_2 \cdot 4\text{H}_2\text{O}$  and by Stout<sup>10</sup> in  $\text{MnF}_2$ . In  $\text{KNiF}_3$ , where  $T_N$  is relatively high, the shift is enhanced and is observed very clearly.

The shift due to spin ordering can be discussed as follows. Let us assume the molecular field approximation where each spin in the crystal is exposed to the effective magnetic field coming from the exchange interaction with the other spins. A simple expression for the effective exchange field  $H_E$  at  $0^\circ\text{K}$  is

$$H_E = 3kT_N/g\mu_B(S+1), \quad (1)$$

where  $\mu_B$  is the Bohr magneton,  $k$  is the Boltzman constant,  $g \approx 2$ , and  $S$  is the effective spin. With  $T_N = 275^\circ\text{K}$  and  $S=1$ ,  $H_E$  for  $\text{KNiF}_3$  turns out to be  $\sim 3 \times 10^6$  Oe. This effective field induces both Zeeman splitting and a small shift of the energy levels: the small shift may be ignored in our problem. The split components of the  ${}^3A_2$  ground state are  $M_s = -1, 0, +1$ . Below room

temperature (also  $< T_N$ ) the  $M_s = 0, +1$  components are almost depopulated, and the transition takes place mainly from the lowest  $M_s = -1$  component whose energy is lowered by  $2\mu_B H_E$  compared to the energy of the unsplit  ${}^3A_2$  level. This corresponds to taking account of the purely spin-antiparallel ground state which is stabilized by antiferromagnetic interactions.

In order to discuss the frequency shift in the optical spectrum, we have to know the effect of magnetic interactions on the excited states as well as the selection

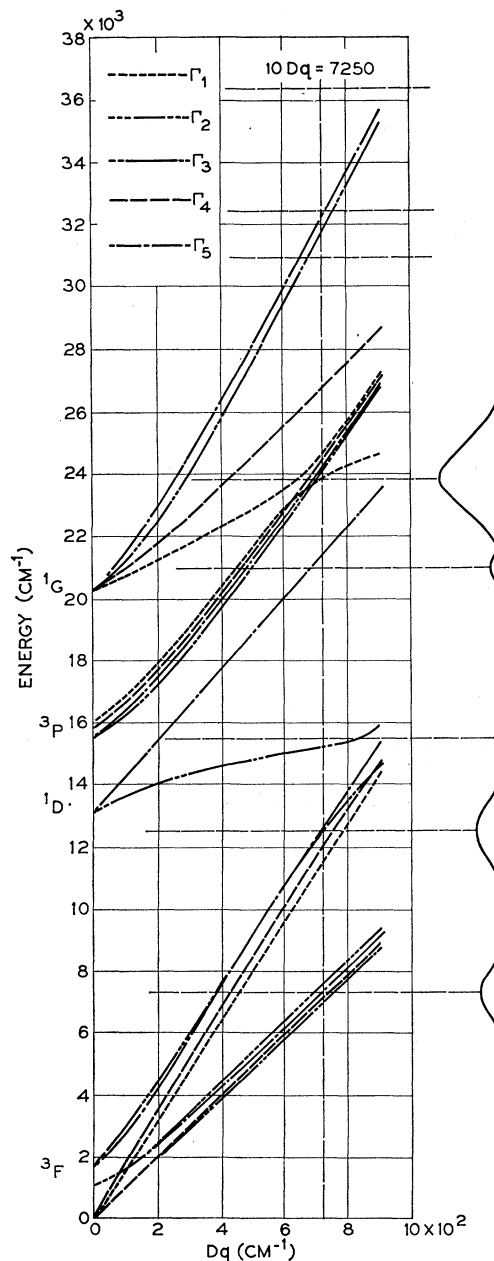


FIG. 5. Plot of Liehr and Ballhausen's calculation of the energy levels of  $\text{Ni}^{2+}$  in cubic fields vs our observed spectrum. We have used their calculation for  $F_2 = 14F_4 = 1540 \text{ cm}^{-1}$  and  $\lambda = -250 \text{ cm}^{-1}$ .

<sup>9</sup> I. Tsujikawa, J. Phys. Soc. Japan 13, 315 (1958).

<sup>10</sup> J. W. Stout, J. Chem. Phys. 31, 709 (1959).

rules of optical transitions. When the molecular field approximation is used for the excited states, the Zeeman splitting can, in principle, be known. The excited spin triplets are orbitally degenerate (accordingly the orbital angular momentum is unquenched), so that the Zeeman levels are not specified by  $M_s$  but a quantum number similar to  $M_J$ . This means that the spin-antiparallel state considered in the ground state is no longer a pure quantum state in the excited states and mixes into several components split by magnetic interactions. This weakens the selection rule derived from a simple spin-only consideration. Furthermore, the situation becomes more complicated because first the vibronic interactions in the degenerate states destroy the quantum number similar to  $M_J$ ,<sup>11,12</sup> and second the transitions are parity forbidden but slightly allowed by excitation of specific phonons.<sup>13</sup> Such complicated circumstances allow transitions from the  $M_s = -1$  ground state to more Zeeman levels of the excited states than expected. Therefore, we suggest that the magnetic interactions in the excited states give smaller contributions to the frequency shift than those in the ground state. Actually the average additional shift in  $\text{KNiF}_3$  below  $T_N$  is  $\sim 300 \text{ cm}^{-1}$  which is close to the simple contribution of the ground state,  $2\mu_B H_E$  where  $H_E \sim 3 \times 10^6 \text{ Oe}$ .

The origin of the shift of the  ${}^3A_2 \rightarrow {}^1E$  band can more clearly be understood, since the Zeeman splitting of the  ${}^1E$  state is very small as shown in the following subsection. The shift in this case is ascribed simply to the antiferromagnetic stabilization of the ground state. The observed shift,  $320 \text{ cm}^{-1}$ , is in good agreement with the theoretical prediction,  $2\mu_B H_E$ .

### C. An Extra Line in the ${}^3A_2 M {}^1E$ Band

A puzzle in our spectroscopic study arises from the behavior of the  ${}^3A_2 \rightarrow {}^1E$  band, especially from the

<sup>11</sup> W. Moffitt and A. D. Liehr, *Phys. Rev.* **106**, 1195 (1957).

<sup>12</sup> H. C. Longuet-Higgins, U. Öpik, M. H. L. Pryce, and R. A. Sack, *Proc. Roy. Soc. (London)* **A244**, 1 (1958).

<sup>13</sup> S. Sugano, *Suppl. Prog. Theoret. Phys. (Kyoto)* **14**, 66 (1960).

appearance of an extra line below  $T_N$  at the higher frequency side separated by  $\sim 300\text{--}400 \text{ cm}^{-1}$  from the main line in the paramagnetic state. The absence of this extra line in the dilute crystal indicates that it is associated with the magnetic ordering.

Within the molecular field approximation, we have been unable to explain the appearance of the two peaks with several hundred  $\text{cm}^{-1}$  separation. As mentioned previously, at low temperatures the electrons populate the lowest component of the ground state almost exclusively. Accordingly, the two peaks must be ascribed to the splitting of the  ${}^1E$  excited state if we assume that they arise from purely electronic transitions. It is certainly possible for the effective magnetic field  $H_E$  to split the  ${}^1E$  level as seen from the term,  $\beta H_E g_0 T(A_2)$ , in Tanabe and Kamimura's<sup>14</sup> effective Hamiltonian. The splitting is third order in the perturbation calculation, in which the spin-orbit interaction enters twice. The splitting,  $\Delta E$ , is given by

$$\Delta E \approx \lambda^2 \mu_B H_E / \Delta W^2,$$

where  $\Delta W$  is the energy separation between the  ${}^1E$  and  ${}^3T_1$  levels. Inserting  $\lambda = 250 \text{ cm}^{-1}$ ,  $\Delta W = 3000 \text{ cm}^{-1}$ , and  $H_E = 3 \times 10^6 \text{ Oe}$ , we obtain  $\Delta E \approx 2 \text{ cm}^{-1}$  which is too small to explain the observed separation of the two peaks.

The observed temperature dependence of the extra line reminds us of Newman and Chrenko's experiment<sup>15</sup> on the absorption line located at 0.24 eV in NiO. The NiO crystal is antiferromagnetic below  $640^\circ\text{K}$  and the 0.24-eV line appears just below this temperature. When the temperature is decreased from  $T_N$ , the line intensity increases, the linewidth decreases, and the peak shifts towards higher frequencies. This behavior is quite similar to that of the extra line observed in  $\text{KNiF}_3$ . We are continuing to investigate the origin of this line.

<sup>14</sup> Y. Tanabe and H. Kamimura, *J. Phys. Soc. Japan* **13**, 394 (1958).

<sup>15</sup> R. Newman and R. M. Chrenko, *Phys. Rev.* **114**, 1507 (1959).